PCCP

PAPER

View Article Online
View Journal | View Issue

Cite this: *Phys. Chem. Chem. Phys.*, 2019, **21**, 5655

Ice Ih *vs.* ice III along the homogeneous nucleation line

Jorge R. Espinosa,[a] Angel L. Diez,[a] Carlos Vega,[a] Chantal Valeriani,[b] Jorge Ramirez[c] and Eduardo Sanz[a]

Received 4th December 2018,
Accepted 12th February 2019

DOI: 10.1039/c8cp07432a

rsc.li/pccp

Pure water can be substantially supercooled below the melting temperature. The pressures and temperatures where water is observed to freeze in supercooling experiments define the so-called homogeneous nucleation line. The slope of such a line changes from negative to positive as pressure increases. In our work, we use computer simulations with the TIP4P/Ice water model to investigate such a change of slope. The simulation prediction for the melting and the homogeneous nucleation lines is in reasonable agreement with the experiment. We find, in accordance with a previous hypothesis, that the aforementioned slope sign inversion can be explained by a change in the nucleating ice polymorph from ice Ih to ice III. Moreover, we underline the kinetic character of the homogeneous nucleation line by defining different lines for different values of the nucleation rate. We analyse in detail the factors that affect the competition between ices Ih and III in the framework of classical nucleation theory.

Understanding water freezing has strong implications in climate change prediction,[1–3] cryopreservation,[4] and planetary and atmospheric science.[2,5,6] The simplest conceivable freezing-mechanism is the homogeneous nucleation of ice from supercooled water. Although ice formation predominantly occurs heterogeneously,[2,7] it is likely that homogeneous ice nucleation from nearly pure water occurs in clean atmospheric conditions (upper troposphere).[8–11] In addition, heterogeneous nucleation and crystallization from solution cannot be rationalised without having fully understood homogeneous nucleation first.[12–14]

Understanding homogeneous ice nucleation in compressed water is relevant for high pressure cooling in the preservation of food and biological samples.[4,15,16] Moreover, the freezing behaviour at high pressures can provide clues to obtain amorphous water[17–19] or to probe water in the so-called no man's land.[19–22]

In 1975, Kanno, Speedy and Angell conducted a pioneering study of homogeneous ice nucleation at high pressures.[23] By cooling emulsified microscopic water drops at different pressures, they established the so-called homogeneous nucleation line (HNL),[23] which corresponds to the loci in the (p,T) plane where the drops were observed to freeze. In the absence of impurities, freezing occurs well below the melting temperature (T_m) because the birth of ice requires surmounting a free energy barrier due to the appearance of an interface between the emerging solid nucleus and the surrounding liquid.[23–26] For instance, Kanno, Speedy and Angell found that the freezing temperature is 42 K below T_m at 1 bar.

The experimental HNL is shown with a thin solid black line in Fig. 1. The black thick solid lines in the figure indicate the ice–liquid coexistence; solid and dashed lines correspond to the melting of ices Ih and III, respectively. The parallelism between the melting and the homogeneous nucleation lines suggests that the kink in the HNL corresponds to a change in

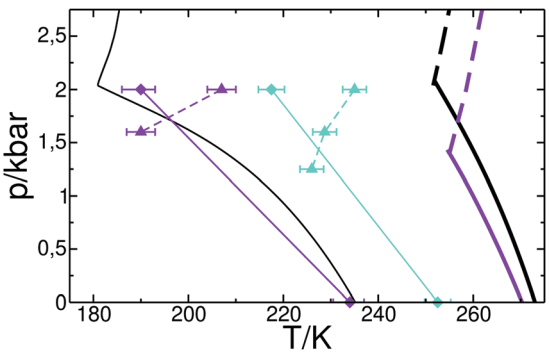

Fig. 1 Melting and HN lines in the p,T plane for experiments (black)[23] and the TIP4P/Ice model (purple). Thick lines correspond to the melting curves of ices Ih (solid) and III (dashed). Thin lines correspond to the HNL. Diamonds (triangles), joined by a solid (dashed) purple line for visual aid, correspond to freezing *via* ice Ih (III). Simulation results for ice Ih were published in previous work,[27] whereas those for ice III are presented here. We show the HNL_{-100} for the TIP4P/Ice model in turquoise (see main text).

[a] *Departamento de Quimica Fisica, Facultad de Ciencias Quimicas, Universidad Complutense de Madrid, 28040 Madrid, Spain*
[b] *Departamento de Estructura de la Materia, Fisica Termica y Electronica, Facultad de Ciencias Fisicas, Universidad Complutense de Madrid, 28040 Madrid, Spain*
[c] *Departamento de Ingenieria Quimica Industrial y Medio Ambiente, Escuela Tecnica Superior de Ingenieros Industriales, Universidad Politecnica de Madrid, 28006 Madrid, Spain*

the nucleating phase from ice Ih to ice III.[26] This hypothesis has not been confirmed yet, because experiments do not have access to the structure of the critical crystal nucleus. The aim of this paper is to test if the HNL kink can be justified by the involvement of ice III in water freezing. This not a trivial task. In fact, only recently, we proposed that the part of the HNL with negative slope is explained by freezing *via* ice Ih nuclei[27] rather than *via* other metastable ice polymorphs.[28]

We use the TIP4P/Ice water model[29] to reach our objective. Recently, we have computed the HNL for this model considering ice Ih up to 2 kbar (corresponding to the part of the HNL with a negative slope).[27] The model predictions for melting and HN lines, both considering ice Ih, are in fairly good agreement with the experiment (solid purple *vs.* solid black lines in Fig. 1). Our simulations with TIP4P/Ice enabled us to predict that the temperature difference between the ice Ih melting and HN lines increases with pressure due to an increase of the ice Ih–liquid interfacial free energy.[27] So far, we have restricted our work to ice Ih. To test the hypothesis that the change in slope of the HNL corresponds to a change in the nucleating phase (from ice Ih to ice III), we compute the melting and the HN lines of ice III. All results in this paper regarding ice Ih have been previously published,[27,30] whereas those corresponding to ice III are presented here for the first time.

We compute the ice III melting line by direct coexistence,[31,32] which consists in simulating the solid and the liquid at contact in the *NpT* ensemble at several temperatures. Below melting the solid grows and above it melts. Thus, we enclose the melting temperature within a certain temperature range. This technique properly takes into account the orientational disorder of water molecules in the ice structure.[33] The resulting melting line is shown as a thick purple dashed line in Fig. 1. Although the agreement with the experiment is not perfect, the model captures quite well the experimental features of the melting curves.

Next, we need to obtain the HNL for ice III. It is important to note that the position of the HNL depends on the sample volume, V, and on the cooling rate.[13,27] More specifically, the rate probed at the HNL is given by $1/(t_c V)$,[27] where t_c is the time spent at each Celsius degree. This ratio takes values of 10^{16} m^{-3} s^{-1} in typical experiments of microscopic drops where the temperature drops a Kelvin every 10–20 seconds (t_c = 10–20 s).[13,27,34–42] Therefore, we need to evaluate the rate as a function of temperature, $J(T)$, for different pressures in order to locate the HNL.

Because ice nucleation is a rare event, obtaining the rate as a function of pressure and temperature is a highly demanding task from a computational point of view.[43] For instance, obtaining the ice nucleation rate of TIP4P/Ice at a single state point with Forward Flux Sampling[44] took tens of millions of CPU hours.[43] To locate the HNL we need the rate not just for a single state point, but for a wide range of pressures and temperatures. Therefore, we cannot use rigorous rare event techniques.[44–48] We resort to the approximate seeding technique, that combining simulations with classical nucleation theory[49–53] has proven able to give the correct rate trends for a variety of systems: hard spheres, Lennard-Jones, mW water and Tosi–Fumi NaCl.[51,54] The name of "Seeding" comes from the fact that one needs to simulate ice seeds embedded in supercooled water. In previous work we computed the nucleation rate as a function of temperature for two different pressures using ice Ih seeds.[27,30]

Here, we apply to ice III the same sort of calculations as those described in ref. 27 and 30 to obtain the nucleation rate *via* ice Ih seeds. The simulation details are exactly the same, so we omit them here to avoid redundancy. The only details specific to the new work we present here are the way ice III seeds were generated and detected. To build an ice III seed with proper orientational disorder we let ice III spontaneously grow in a direct coexistence simulation and cut a spherical seed from the grown solid. To detect ice III we use an averaged[55] Steinhardt-like order parameter.[56] In particular, we compute for each particle a $\bar{q}_6$ order parameter (see ref. 51) with a distance of 4.83 Å to identify neighbors. The $\bar{q}_6$ threshold to establish if a molecule belongs to a solid or a liquid environment weakly depends on temperature and pressure and is obtained with the mislabelling criterion as explained in ref. 51.

To obtain the ice III nucleation rate and, henceforth, the HNL we used three different seeds (of about 8000, 3000 and 500 molecules) at three different pressures. The supercooling (temperature difference with respect to melting) at which the inserted ice III nuclei were found to be critical in our seeding simulations is plotted in Fig. 2. For a given supercooling, the critical cluster size, N_c, does not vary much with pressure. As we show below, this is due to the fact that, for a given supercooling, neither the chemical potential difference between the solid and the fluid nor the interfacial free energy between both phases change much with pressure for the case of ice III.

With the N_c data shown in Fig. 2 one can get fits for the nucleation rate as a function of temperature at different pressures as explained in ref. 51. In particular, we use the classical nucleation theory expression for the rate, J:[24,57,58]

$$J = A \exp(-\Delta G_c/(k_B T)) \quad (1)$$

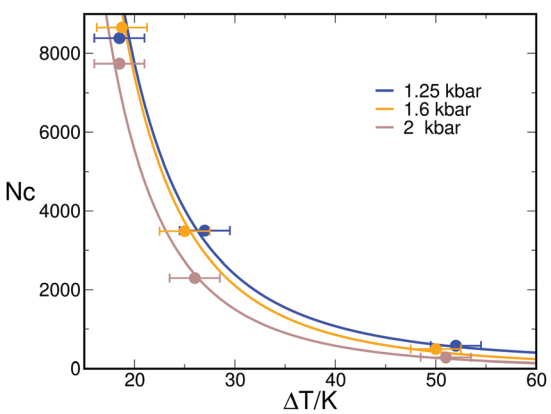

Fig. 2 Critical cluster size, N_c, *versus* supercooling, ΔT, for ice III at different pressures. Points correspond to seeding simulations whereas lines are fits based on classical nucleation theory.[51]

where A is a kinetic pre-factor and ΔG_c is the work required to reversibly form the critical cluster at constant p and T. Assuming a spherical critical cluster,[59] ΔG_c is given by:

$$\Delta G_c(T) = \frac{16\pi(\gamma(T))^3}{3(\rho_s(T))^2|\Delta\mu(T)|^2} \quad (2)$$

where, ρ_s is the solid density, γ is the ice–liquid interfacial free energy and $\Delta\mu$ is the solid–liquid chemical potential difference.

In what follows we analyse the influence of ρ_s, $\Delta\mu$, γ and A in the competition between both polymorphs on water freezing.

Regarding the solid density, it is about 0.93 and 1.15 g cm^{-3} for ices Ih and III, respectively. Since $\rho_s{}^2$ appears in the denominator of the expression for ΔG_c (eqn (2)), ice III will be favoured with respect to ice Ih. Specifically, the barrier for nucleating ice Ih will be about 1.5 times larger due to the solid density effect.

$|\Delta\mu|$ is obtained *via* thermodynamic integration from the melting temperature.[51] For a given supercooling, $|\Delta\mu|$ does not change significantly with either pressure or with the ice polymorph (see Fig. 3 where we show $|\Delta\mu|$ *versus* ΔT for both ice polymorphs and all pressures studied). The $|\Delta\mu|$ curves become somewhat different at large supercooling, but this does not affect much the location of the HNLs. Then, regarding $|\Delta\mu|$, the competition between both ice polymophs depends on the temperature difference with respect to the corresponding melting line. In other words, unsurprisingly, the nucleation of an ice polymorph is favoured where it is the most stable phase. This explains why, as shown below, the competition between both polymorphs occurs at pressures close to the liquid–ice Ih–ice III triple point pressure.

We obtain γ *via* CNT as:

$$\gamma = \left(\frac{3N_c\rho_s{}^2|\Delta\mu|^3}{32\pi}\right)^{1/3}, \quad (3)$$

where, ρ_s is the solid density. Thus, we obtain a value of γ for each ice III inserted cluster. As in the previous work for ice Ih,[27,30,50] we find a linear dependence of γ with temperature. The linear fits to $\gamma(T)$ for both ice polymorphs and all studied pressures are shown in Fig. 4. For a given temperature, γ increases with pressure for ice Ih, whereas it either slightly decreases or remains constant for ice III, within a 10 percent error in our γ estimates. Then, increasing pressure will favor ice III in what is regarded the interfacial free energy.

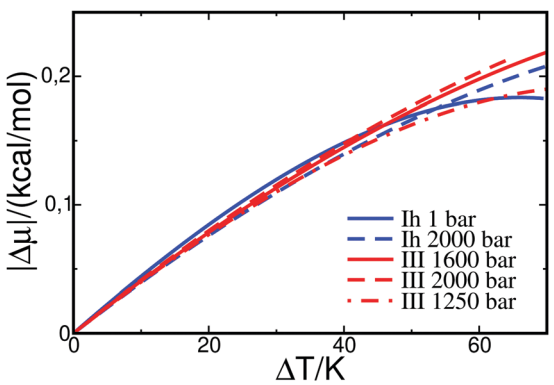

Fig. 3 Chemical potential difference between the liquid and either ice Ih (blue, ref. 27 and 30) or ice III (red, this work) at different pressures (see legend) as a function of the supercooling.

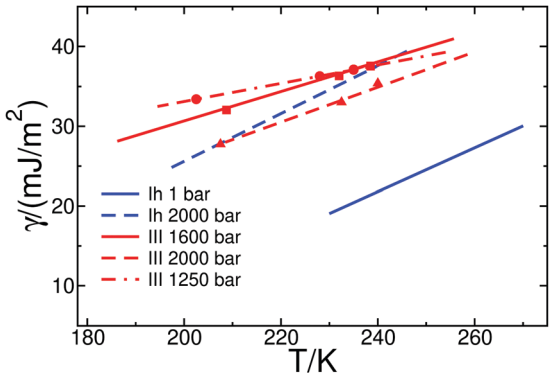

Fig. 4 Ice–liquid interfacial free energy as a function of temperature for ices Ih (blue, ref. 27 and 30) and III (red, this work) at different pressures. Symbols correspond to ice III–liquid γ estimates obtained from seeding simulations and eqn (3) (circles, squares and triangles correspond to 1.25, 1.6 and 2 kbar, respectively). Lines are linear fits to the data obtained from seeding. For ice Ih we published elsewhere the seeding data[27] and we only show the linear fits.

The kinetic pre-factor A is obtained as in the previous work *via* the following CNT expression:[51]

$$A = \rho_f\sqrt{\frac{|\Delta\mu|}{6\pi k_B T N_c}}f^+ \quad (4)$$

where ρ_f is the liquid density and f^+ is the frequency with which molecules attach to the critical cluster. f^+ can be obtained in simulations as suggested in ref. 60. In our previous work for ice Ih,[27,30] and here for a couple of ice III clusters, we have checked that the approach proposed in ref. 60 to compute f^+ is consistent with the following CNT expression for $\lambda \sim 1$ molecular diameter:

$$f^+ = \frac{24DN^{2/3}}{\lambda^2} \quad (5)$$

where D is the liquid diffusion coefficient. Using the above two equations we obtain, at 2 kbar, a kinetic pre-factor A ranging from $10^{37\pm1}$ m^{-3} s^{-1} at low T to $10^{39\pm1}$ m^{-3} s^{-1} at high T for both ice polymorphs. To understand why the kinetic pre-factor is similar for both ice polymorphs we look at their ratio, which according to the expressions (3)–(5) is given by:

$$\frac{A_{III}}{A_{Ih}} = \sqrt{\frac{\gamma_{III}}{\gamma_{Ih}}}\left(\frac{\rho_{s,Ih}}{\rho_{s,III}}\right)^{1/3} \quad (6)$$

Since, for 2000 bar γ_{III} is similar to γ_{Ih} (see Fig. 4) and the solid densities are also comparable, it is understandable that the kinetic pre-factors are close to each other. It is expected that the analysis performed here for 2 kbar will not be that different for any other pressure in the range of 1.5–2 kbar where both polymorphs compete (close to the liquid–ice Ih–ice III triple pressure).

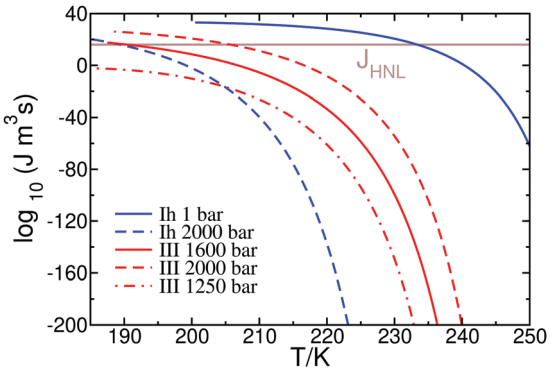

Fig. 5 Nucleation rate as a function of temperature for ices Ih (blue, ref. 27 and 30) and III (red, this work) at different pressures.

Perhaps, our data in Fig. 4 suggests that for pressures lower than 2 kbar γ_{III} is larger than γ_{Ih}. Then, the kinetic pre-factor for ice III is expected to be higher than that of ice Ih at pressures lower than 2 kbar. However, the difference will not be larger than one order of magnitude, which is not going to significantly shift the location of the HNLs. In summary, the kinetic pre-factor does not play a key role in the competition between both ice polymorphs.

With the temperature dependence at different pressures of ρ_s, $|\Delta\mu|$, γ and A we can obtain fits for the nucleation rate at three different pressures. Results for ice III at 1.25, 1.6 and 2 kbar are shown in red in Fig. 5. The fits for the nucleation rate *via* ice Ih seeds at two different pressures are shown in blue in Fig. 5 (these results are taken from ref. 27 and 30). The horizontal line in Fig. 5 corresponds to the rate that is probed at the experimental HNL (10^{16} m^{-3} s^{-1}). Therefore, the crossings between the horizontal line and the rate curves define points of the HNL for each polymorph. The ice III 1.25 kbar rate curve does not reach 10^{16} m^{-3} s^{-1}; so we only obtained points for the ice III HNL from the 1.6 and 2 kbar isobars. The HNL points thus found are plotted in Fig. 1 with purple diamonds and triangles for ices Ih and III, respectively. Although the HNL could have some curvature, lines joining these points roughly indicate where the HNL for each polymorph lies. Obviously, for a given pressure, the HNL that lies at higher temperature will determine the phase that is formed on cooling water. The ice Ih and ice III HNLs cross at around 1.7 kbar and 196 K. Therefore, the model prediction is that ice Ih will nucleate on cooling water drops below 1.7 kbar and ice III will be formed at higher pressures. The resemblance between the simulation and the experimental HNLs is quite evident. This suggests that, indeed, the change in slope in the experimental HNL is due to a change in the nucleating phase, which is the main conclusion we draw from our study.

A due comment here is that the HNL is a kinetic and not a thermodynamic line. The HNL defined so far corresponds to the loci in the (p–T) plane where the rate is 10^{16} m^{-3} s^{-1}. We now define another homogeneous nucleation line, HNL_{-100}, as that given by a rate of 10^{-100} m^{-3} s^{-1}. Although such rate is not accessible experimentally,[50] defining the HNL_{-100} serves for our purpose of illustrating that the freezing line is indeed a kinetic one. This academic exercise requires obtaining $J(T)$ for a wide temperature range, a task that is nowadays only accessible to seeding simulations. The HNL_{-100} is shown in turquoise in Fig. 1 (diamonds joined by solid lines correspond to nucleation *via* ice Ih whereas triangles joined by dashed lines correspond to ice III). The HNL_{-100} is significantly shifted with respect to the HNL defined for $J = 10^{16}$ m^{-3} s^{-1} (in purple), which shows the kinetic character of the freezing line. The HNL_{-100}s for ice III and ice Ih cross at 1.4 kbar and 227 K (*versus* 1.7 kbar and 196 K for $J = 10^{16}$ m^{-3} s^{-1}). Obviously, the HNL_{-100} is shifted to higher temperatures because ice forms at lower rates in warmer water. The shift of the crossing point from 1.7 to 1.4 kbar is not so obvious because, as discussed above, the competition between both polymorphs depends on a balance between densities, chemical potentials and interfacial free energies.

In summary, we have used the seeding technique to evaluate the HNL for the TIP4P/Ice water model. Both the melting and the HN lines of the model are in reasonable quantitative agreement with the real ones. As pressure increases, the slope of the HNL changes from negative to positive at a pressure close to that of the liquid–ice Ih–ice III triple point. This slope switch corresponds to a change in the structure of the emerging nucleus from ice Ih to ice III, which is the main conclusion of our work. We show that the location of the HNL depends on the nucleation rate for which the HNL is defined. This underlines the kinetic character of the HNL. To conclude, we summarize the factors that affect the competition between both polymorphs as follows: the kinetic pre-factor is not decisive, the solid density favors ice III at any pressure, the chemical potential difference favors the stable phase and pressure favors ice III because its interfacial free energy does not vary much with pressure whereas that of ice Ih increases with pressure.

Conflicts of interest

There are no conflicts to declare.

Acknowledgements

This work was funded by grant FIS2016/78117-P of the MEC. The authors acknowledge the computer resources and technical assistance provided by RES and the Centro de Supercomputacion y Visualizacion de Madrid (CeSViMa).

References

1 M. B. Baker, Cloud microphysics and climate, *Science*, 1997, **276**, 1072–1078.
2 W. Cantrell and A. Heymsfield, Production of ice in tropospheric clouds, *Bull. Am. Meteorol. Soc.*, 2005, **86**, 795.
3 P. J. DeMott, A. J. Prenni, X. Liu, S. M. Kreidenweis, M. D. Petters, C. H. Twohy, M. S. Richardson, T. Eidhammer and

D. C. Rogers, Predicting global atmospheric ice nuclei distributions and their impacts on climate, *Proc. Natl. Acad. Sci. U. S. A.*, 2010, **107**, 11217–11222.
4 G. J. Morris and E. Acton, Controlled ice nucleation in cryopreservation-a review, *Cryobiology*, 2013, **66**, 85.
5 P. Jenniskens, D. F. Blake, M. A. Wilson and A. Pohorille, High-Density Amorphous Ice, the Frost on Interstellar Grains, *Astrophys. J.*, 1995, **455**, 389.
6 G. C. Sosso, J. Chen, S. J. Cox, M. Fitzner, P. Pedevilla, A. Zen and A. Michaelides, Crystal nucleation in liquids: open questions and future challenges in molecular dynamics simulations, *Chem. Rev.*, 2016, **116**(12), 7078–7116.
7 B. J. Murray, D. O'Sullivan, J. D. Atkinson and M. E. Webb, Nucleation by particles immersed in supercooled cloud droplets, *Chem. Soc. Rev.*, 2012, **41**, 6519–6554.
8 G. De Boer, H. Morrison, M. Shupe and R. Hildner, Evidence of liquid dependent ice nucleation in high-latitude stratiform clouds from surface remote sensors, *Geophys. Res. Lett.*, 2011, **38**(1), L01803.
9 Y.-S. Choi, R. S. Lindzen, C.-H. Ho and J. Kim, Space observations of cold-cloud phase change, *Proc. Natl. Acad. Sci. U. S. A.*, 2010, **107**(25), 11211–11216.
10 C. D. Westbrook and A. J. Illingworth, Evidence that ice forms primarily in supercooled liquid clouds at temperatures > -27 °C, *Geophys. Res. Lett.*, 2011, **38**(14), L14808.
11 D. Rosenfeld and W. L. Woodley, Deep convective clouds with sustained supercooled liquid water down to -37.5 °C, *Nature*, 2000, **405**(6785), 440.
12 D. H. Rasmussen, Ice formation in aqueous systems, *J. Microsc.*, 1982, **128**(2), 167–174.
13 T. Koop, B. Luo, A. Tsias and T. Peter, Water activity as the determinant for homogeneous ice nucleation in aqueous solutions, *Nature*, 2000, **406**, 611–614.
14 D. Turnbull, Kinetics of heterogeneous nucleation, *J. Chem. Phys.*, 1950, **18**(2), 198–203.
15 D. Studer, *High-pressure freezing system*, *US Pat.* 6,269,649, Aug. 7 2001.
16 P. C. Myint, A. A. Chernov, B. Sadigh, L. X. Benedict, B. M. Hall, S. Hamel and J. L. Belof, Nanosecond freezing of water at high pressures: nucleation and growth near the metastability limit, *Phys. Rev. Lett.*, 2018, **121**(15), 155701.
17 G. M. Fahy, B. Wowk, J. Wu, J. Phan, C. Rasch, A. Chang and E. Zendejas, Cryopreservation of organs by vitrification: perspectives and recent advances, *Cryobiology*, 2004, **48**(2), 157–178. Special issue: Keynote papers from CRYOBIOMOL – 2003.
18 T. Loerting, K. Winkel, M. Seidl, M. Bauer, C. Mitterdorfer, P. H. Handle, C. G. Salzmann, E. Mayer, J. L. Finney and D. T. Bowron, How many amorphous ices are there?, *Phys. Chem. Chem. Phys.*, 2011, **13**, 8783–8794.
19 O. Mishima and H. E. Stanley, The relationship between liquid, supercooled and glassy water, *Nature*, 1998, **396**, 329–335.
20 A. Manka, H. Pathak, S. Tanimura, J. Wolk, R. Strey and B. E. Wyslouzil, Freezing water in no man's land, *Phys. Chem. Chem. Phys.*, 2012, **14**, 4505–4516.
21 F. Caupin, Escaping the no man's land: Recent experiments on metastable liquid water, *J. Non-Cryst. Solids*, 2015, **407**, 441–448.
22 P. H. Poole, F. Sciortino, U. Essmann and H. E. Stanley, Phase behavior of metastable water, *Nature*, 1992, **360**, 324.
23 H. Kanno, R. J. Speedy and C. A. Angell, Supercooling of water to -92 °C under pressure, *Science*, 1975, **189**(4206), 880–881.
24 K. F. Kelton, *Crystal Nucleation in Liquids and Glasses*, Academic, Boston, 1991.
25 P. G. Debenedetti, *Metastable liquids: Concepts and Principles*, Princeton University Press, 1996.
26 P. G. Debenedetti, Supercooled and glassy water, *J. Phys.: Condens. Matter*, 2003, **15**, R1669–R1726.
27 J. R. Espinosa, A. Zaragoza, P. Rosales-Pelaez, C. Navarro, C. Valeriani, C. Vega and E. Sanz, Interfacial free energy as the key to the pressure-induced deceleration of ice nucleation, *Phys. Rev. Lett.*, 2016, **117**, 135702.
28 J. Russo, F. Romano and H. Tanaka, New metastable form of ice and its role in the homogeneous crystallization of water, *Nat. Mater.*, 2014, **13**, 733.
29 J. L. F. Abascal, E. Sanz, R. G. Fernandez and C. Vega, A potential model for the study of ices and amorphous water: TIP4P/Ice, *J. Chem. Phys.*, 2005, **122**, 234511.
30 J. R. Espinosa, C. Navarro, E. Sanz, C. Valeriani and C. Vega, On the time required to freeze water, *J. Chem. Phys.*, 2016, **145**(21), 211922.
31 A. Ladd and L. Woodcock, Triple-point coexistence properties of the Lennard-Jones system, *Chem. Phys. Lett.*, 1977, **51**(1), 155–159.
32 E. G. Noya, C. Vega and E. de Miguel, Determination of the melting point of hard spheres from direct coexistence simulation methods, *J. Chem. Phys.*, 2008, **128**(15), 154507.
33 M. M. Conde, M. A. Gonzalez, J. L. F. Abascal and C. Vega, Determining the phase diagram of water from direct coexistence simulations: The phase diagram of the TIP4P/2005 model revisited, *J. Chem. Phys.*, 2013, **139**(15), 154505.
34 H. R. Pruppacher, A new look at homogeneous ice nucleation in supercooled water drops, *J. Atmos. Sci.*, 1995, **52**, 1924.
35 B. J. Murray, S. L. Broadley, T. W. Wilson, S. J. Bull, R. H. Wills, H. K. Christenson and E. J. Murray, Kinetics of the homogeneous freezing of water, *Phys. Chem. Chem. Phys.*, 2010, **12**, 10380.
36 B. Riechers, F. Wittbracht, A. Hutten and T. Koop, The homogeneous ice nucleation rate of water droplets produced in a microfluidic device and the role of temperature uncertainty, *Phys. Chem. Chem. Phys.*, 2013, **15**, 5873–5887.
37 P. Stockel, I. M. Weidinger, H. Baumgartel and T. Leisner, Rates of homogeneous ice nucleation in levitated H_2O and D_2O droplets, *J. Phys. Chem. A*, 2005, **109**(11), 2540–2546.
38 C. A. Stan, G. F. Schneider, S. S. Shevkoplyas, M. Hashimoto, M. Ibanescu, B. J. Wiley and G. M. Whitesides, A microfluidic apparatus for the study of ice nucleation in supercooled water drops, *Lab Chip*, 2009, **9**, 2293–2305.
39 B. Kramer, O. Hubner, H. Vortisch, L. Woste, T. Leisner, M. Schwell, E. Ruhl and H. Baumgartel, Homogeneous

nucleation rates of supercooled water measured in single levitated microdroplets, *J. Chem. Phys.*, 1999, **111**(14), 6521–6527.

40 D. Duft and T. Leisner, Laboratory evidence for volume-dominated nucleation of ice in supercooled water microdroplets, *Atmos. Chem. Phys.*, 2004, **4**(7), 1997–2000.

41 D. Rzesanke, J. Nadolny, D. Duft, R. Muller, A. Kiselev and T. Leisner, On the role of surface charges for homogeneous freezing of supercooled water microdroplets, *Phys. Chem. Chem. Phys.*, 2012, **14**, 9359–9363.

42 S. Benz, K. Megahed, O. Möhler, H. Saathoff, R. Wagner and U. Schurath, T-dependent rate measurements of homogeneous ice nucleation in cloud droplets using a large atmospheric simulation chamber, *J. Photochem. Photobiol., A*, 2005, **176**(1–3), 208–217.

43 A. Haji-Akbari and P. G. Debenedetti, Direct calculation of ice homogeneous nucleation rate for a molecular model of water, *Proc. Natl. Acad. Sci. U. S. A.*, 2015, **112**(34), 10582–10588.

44 R. J. Allen, P. B. Warren and P. R. Ten Wolde, Sampling rare switching events in biochemical networks, *Phys. Rev. Lett.*, 2005, **94**, 018104.

45 J. S. van Duijneveld and D. Frenkel, Computer simulation study of free energy barriers in crystal nucleation, *J. Chem. Phys.*, 1992, **96**, 4655.

46 F. Trudu, D. Donadio and M. Parrinello, Freezing of a Lennard-Jones fluid: from nucleation to spinodal regime, *Phys. Rev. Lett.*, 2006, **97**, 105701.

47 D. Moroni, P. R. ten Wolde and P. G. Bolhuis, Interplay between structure and size in a critical crystal nucleus, *Phys. Rev. Lett.*, 2005, **94**, 235703.

48 S. Pipolo, M. Salanne, G. Ferlat, S. Klotz, A. M. Saitta and F. Pietrucci, Navigating at will on the water phase diagram, *Phys. Rev. Lett.*, 2017, **119**(24), 245701.

49 B. C. Knott, V. Molinero, M. F. Doherty and B. Peters, Homogeneous nucleation of methane hydrates: unrealistic under realistic conditions, *J. Am. Chem. Soc.*, 2012, **134**, 19544–19547.

50 E. Sanz, C. Vega, J. R. Espinosa, R. Caballero-Bernal, J. L. F. Abascal and C. Valeriani, Homogeneous ice nucleation at moderate supercooling from molecular simulation, *J. Am. Chem. Soc.*, 2013, **135**(40), 15008–15017.

51 J. R. Espinosa, C. Vega, C. Valeriani and E. Sanz, Seeding approach to crystal nucleation, *J. Chem. Phys.*, 2016, **144**, 034501.

52 N. E. R. Zimmermann, B. Vorselaars, D. Quigley and B. Peters, Nucleation of NaCl from aqueous solution: critical sizes, ion-attachment kinetics, and rates, *J. Am. Chem. Soc.*, 2015, **137**(41), 13352–13361.

53 N. E. Zimmermann, B. Vorselaars, J. R. Espinosa, D. Quigley, W. R. Smith, E. Sanz, C. Vega and B. Peters, NaCl nucleation from brine in seeded simulations: sources of uncertainty in rate estimates, *J. Chem. Phys.*, 2018, **148**(22), 222838.

54 J. R. Espinosa, C. Vega, C. Valeriani and E. Sanz, The crystal-fluid interfacial free energy and nucleation rate of NaCl from different simulation methods, *J. Chem. Phys.*, 2015, **142**(19), 194709.

55 W. Lechner and C. Dellago, Accurate determination of crystal structures based on averaged local bond order parameters, *J. Chem. Phys.*, 2008, **129**(11), 114707.

56 P. J. Steinhardt, D. R. Nelson and M. Ronchetti, Bond-orientational order in liquids and glasses, *Phys. Rev. B: Condens. Matter Mater. Phys.*, 1983, **28**, 784–805.

57 M. Volmer and A. Weber, Keimbildung in ubersattigten gebilden, *Z. Phys. Chem.*, 1926, **119**, 277.

58 R. Becker and W. Doring, Kinetische behandlung der keimbildung in ubersattigten dampfen, *Ann. Phys.*, 1935, **416**, 719–752.

59 A. Zaragoza, M. M. Conde, J. R. Espinosa, C. Valeriani, C. Vega and E. Sanz, Competition between ices ih and ic in homogeneous water freezing, *J. Chem. Phys.*, 2015, **143**(13), 134504.

60 S. Auer and D. Frenkel, Prediction of absolute crystal-nucleation rate in hard-sphere colloids, *Nature*, 2001, **409**, 1020.

